Chinese Chemical Letters 34 (2023) 108008

Contents lists available at ScienceDirect

Chinese Chemical Letters

journal homepage: www.elsevier.com/locate/cclet

Rational design of AIE-active biodegradable polycarbonates for high-performance WLED and selective detection of nitroaromatic explosives

Shanshan Huang[a,1], Enhao Wang[b,1], Jialin Tong[a], Guo-Gang Shan[a,*], Shunjie Liu[b,*], Haitao Feng[c], Chao Qin[a,*], Xianhong Wang[b], Zhongmin Su[a]

[a] National & Local United Engineering Laboratory for Power Batteries, Department of Chemistry, Northeast Normal University, Changchun 130024, China
[b] Key Laboratory of Polymer Ecomaterials, Changchun Institute of Applied Chemistry, Chinese Academy of Sciences, Changchun 130022, China
[c] AIE Research Center, Shaanxi Key Laboratory of Phytochemistry, College of Chemistry and Chemical Engineering, University of Arts and Sciences, Baoji 721013, China

ARTICLE INFO

Article history:
Received 4 October 2022
Revised 5 November 2022
Accepted 15 November 2022
Available online 17 November 2022

Keywords:
CO_2 copolymerization
Biodegradable polymer
Aggregation induced-emission
Sensor
White light-emitting diode

ABSTRACT

Luminescent polymers have garnered considerable research attention for their excellent properties and wide range of applications in multi-responsive materials, bioimaging, and photoelectric devices. Thereout, various modulations of polymer structure are often the main approach to obtaining materials with different luminescent colors and functions. However, polymers with biodegradability, tunable color, and efficient emission simultaneously remain a challenge. Herein, we report a feasible strategy to achieve degradable and highly emissive polymers by exquisite combination and interplay of aggregation-induced emission (AIE) unit and environmental-friendly epoxide/CO_2 copolymerization. A series of polycarbonates P-TEP$_x$CN$_y$ ($x = 0$, 1, 2, 4, 30, 120; $y = 0$, 1) were prepared, with emission color changed from blue to yellow by controlling the proportion of two designed AIE-active monomers. Among them, Using P-TCN as emitting layer, high performance white light-emitting diode (WLED) device with an external quantum efficiency (EQE) of 26.09% and CIE coordinates of (0.32, 0.32) was achieved. In addition, the designed polymers can be used as selective sensors for nitroaromatic compounds in their nanoaggregate states.

Polymers, both natural and synthetic, play a ubiquitous role in our daily life because of their wide range of properties with high elasticity and toughness. However, due to improper use and indiscriminate disposal, greater pressure has been placed on the environment. Exploration and development of advanced biodegradable polymer materials have become a hotspot of current research in the field of polymer materials [1–3]. Most biodegradable polymers are designed with the idea that the target polymer chains can be changed to progressively smaller biologically acceptable compounds by hydrolysis [4]. Nowadays, commonly available biodegradable polymers mainly includes poly(L-lactic acid) (PLA) [5,6], polyvinylchloride (PVC) [7], polyamide (PA) [8], polypropylene (PP) [9,10], *etc.* Among them, the copolymerization of carbon dioxide with epoxides to obtain polycarbonates is considered a valid way to synthesize polymer materials with biodegradable properties [11–16]. Darensbourg and co-workers reported the preparation of a highly stereospecific alternating CO_2/epichlorohydrin copolymer, poly(chloropropylene carbonate), using the chiral bifunctional cobalt-salen complex as catalyst, and the enantioselectivity of the resultant (*R*)-configuration copolymer prepared from (*R*)-epichlorohydrin reaches to 94% [17]. Wang *et al.* developed a thermoresponsive CO_2/OEG-functionalized epoxides copolymer, P-MEnGE ($n = 2$, 3) with well-defined structures [11]. The obtained polycarbonates possess well biodegradable as well as fluorescence signal "self-reporting" properties.

Nowadays, luminescent polymers have garnered considerable research attention due to their excellent properties and wide range of applications [18–23]. Generally, the addition of luminescent units to the reaction system as initiators, as mentioned above, is one of the main approaches to endow luminescent properties to polymers. Wang *et al.* designed three D-A-type conjugated polymers through the adjustment of their electron donor moieties and served as multicolored drug carriers for cancer therapy [24]. Bunz *et al.* developed two hyperbranched conjugated polymers and

* Corresponding authors.
E-mail addresses: shangg187@nenu.edu.cn (G.-G. Shan), sjliu@ciac.ac.cn (S. Liu), qinc703@nenu.edu.cn (C. Qin).
[1] These authors contributed equally to this work.

https://doi.org/10.1016/j.cclet.2022.108008
1001-8417/

applied them as fluorescent micelle sensor arrays for detecting and discriminating nitroaromatic analytes efficiently in water [25]. Similar to the conventional fluorescent molecules, however, luminescent polymers undergo aggregation-caused quenching (ACQ) effect in their aggregate states mainly caused by the strong intermolecular interactions [26], which hampers their widespread application in some respects. Numerous studies have been devoted to solving the problem, such as modulating the molecular geometry structures and their stacking pattern [27]. An intriguing aggregation-induced emission (AIE) phenomenon that exactly proves to be counter to the ACQ effect has offered an alternative way to overcome the above shortcomings since it was first reported by Tang *et al.* in 2001 [28]. Luminogens with AIE properties show weak or even no emission in dilute solution but significant fluorescence enhancement could be observed in their aggregated states, which provides a novel platform for the design of high-efficiency solid-state luminescent materials [29–31].

To explore superior luminescent polymer materials with AIE properties, great efforts have been devoted to the design of molecular structures [32,33]. Nowadays, a large amount of AIE-active polymers has been prepared and explored in extensive applications such as multi-responsive materials [34–40], drug delivery [41], photodynamic therapy (PDT) [42–47], and organic light-emitting diodes (OLEDs) [48–52]. Nevertheless, studies on the preparation of polymers with both luminescent and biodegradable properties are still relatively scarce today. Likewise, as is known to all, emission color is regarded as one of the indispensable parameters in assessing the performance of the corresponding luminescent materials. The strategy of how to simply modulate the emission color of biodegradable polymers still remains challenging.

Modulation of the emission color of resulting polymers will be easily regulated by adjusting the proportion of monomers with different emission colors presents simultaneously in the reaction system. Herein, to further enrich the design strategy of AIE-active polymers with biodegradable proprieties, as well as to deeply explore the modulation of emission colors, we developed a series of luminescent polymers containing the same biodegradable polycarbonate backbone but multiple branch chains grafted with different proportions of propylene oxide functionalized tetraphenylethylene (TPE-EP and TPE-EPCN) to endow the polymer with AIE proprieties. Thereof, biodegradable polycarbonates with controllable M_n and strong fluorescence emission intensity were obtained.

To achieve functionalized AIE polycarbonates, two AIE-active monomers TPE-EP and TPE-EPCN are designed. Their synthetic routes are summarized in Supporting information. For the copolymers, TPE-labeled biodegradable polycarbonates are synthesized by living alternating copolymerization of CO_2/propylene oxide (PO) using SalenCo(III)Cl/PPNCl catalyst system, which has been confirmed as a highly efficient catalyst system for catalyzing the quantitative conversion of CO_2 and epoxides. Tetraphenylethylene

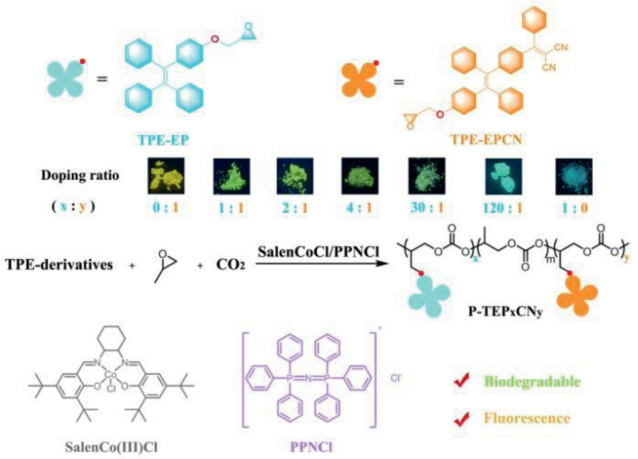

Scheme 1. Preparation of TPE-labeled biodegradable polycarbonates.

derivatives were selected as the major monomers to endow the polymer AIE characteristics to obtain excellent fluorescence emission in the aggregated state. As shown in Scheme 1, two kinds of monomer, TPE-EP and TPE-EPCN with different luminescent colors were utilized to modulate the emission of polycarbonates. The results of copolymerization of CO_2 with the two monomers are summarized in Table 1. All the polymerization reactions were carried out with the corresponding doping ratios of the two monomers in 0.5 mL PO and 0.5 mL toluene, at 30 °C, under 3.0 MPa pressure of CO_2. The reaction time has been optimized to 24 h to ensure the complete conversion of the monomer (the conversion rate exceeds 99%). As shown in entries 1–7 of Table 1, a series of comparatively narrow molar mass dispersion ($Đ$) AIE-active polycarbonates named P-TEP$_x$CN$_y$ ($x = 0$, 1, 2, 4, 30, 120; $y = 0$, 1), where x represents the proportion of TPE-EP and y for TPE-EPCN units in the pendent branch chains were prepared. Their 99% carbonate unit (CU) content indicates that they maintain almost complete alternating copolymerization characteristics. For entries 3–7, the emission color of these polycarbonates under 365 nm UV lamp gradually changed from orange to blue as x:y varied from 1:1 to 120:1. To sum up, well-defined biodegradable polycarbonates with tetraphenylethylene derivative side chains were successfully developed.

Chemical structures of the corresponding polymers with different M_n are well characterized by ^{1}H NMR, ^{13}C NMR, matrix-assisted laser desorption/ionization time-of-flight mass spectroscopy and gel permeation chromatography (GPC) with satisfactory results. The detailed experimental processes and characterization data are summarized in Figs. S1-S9 and S17 (Supporting information). As shown in Figs. 1a and b, the characteristic signals

Table 1
SalenCoCl/PPNCl-catalyzed copolymerization reaction of epoxide/CO_2 with tetraphenylethylene derivatives.

Entry[a]	mono	Conv. (%)	Proportion[d]	Polymer (%)[e]	CU (%)[f]	M_n (g/mol)	PDI
1	x[b]	> 99	–	95	> 99	19,500	1.13
2	y[c]	> 99	–	94	> 99	21,000	1.12
3	x:y	> 99	1:1	96	> 99	23,100	1.11
4	x:y	> 99	2:1	96	> 99	19,700	1.15
5	x:y	> 99	4:1	96	> 99	21,100	1.16
6	x:y	> 99	30:1	96	> 99	20,400	1.10
7	x:y	> 99	120:1	96	> 99	21,800	1.11

[a] The polymerization reactions were carried out in 0.5 mL PO and 0.5 mL toluene, at 30 °C, under 3 MPa CO_2.
[b] *x* represents for TPE-CN.
[c] *y* represents for TPE-EPCN.
[d] The proportion of monomer: TPE-CN and TPE-EPCN in P-TEP$_x$CN$_y$ ($x = 0$, 1, 2, 4, 30, 120; $y = 0$, 1).
[e] Selectivity of polycarbonate to cyclic carbonate.
[f] Content of polycarbonate in the structure.

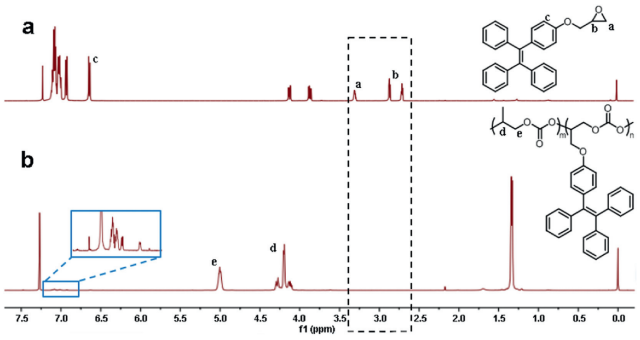

Fig. 1. ^{1}H NMR spectra of (a) TPE-EP and (b) P-TEP in $CDCl_3$.

at δ 6.66–7.17 ppm which ascribes to aromatic protons of TPE-EP could be observed in polycarbonate P-TEP. The strong signals at δ 5.01 and 4.08–4.30 were attributed to CH and CH_2 units in carbonate parts. Meanwhile, the characteristic peaks at δ 3.35–3.31, 2.90–2.88, 2.73–2.74 ppm that correspond to CH_3 and CH, respectively in the oxirane group of TPE-EP, disappeared in polycarbonate P-TEP, and the hydrogen protons adjacent to the oxirane group at δ 4.24 ppm shifted to a lower field, 4.35 ppm, after polymerization, implying the successful connection to the polymer backbone of TPE unit.

In addition, characteristic peaks put down to the ether group (homopolymer of epoxides, appears at δ 3.30–3.60 ppm) did not appear, suggesting the alternative architecture of the backbone of P-TEP (CU content >99%). This also applies to P-TEP$_x$CN$_y$ ($x = 1$, 2, 4, 30, 120; $y = 1$) and P-TCN (Figs. S10-S16 in Supporting information). The emission and absorption behavior of TPE-EPCN, TPE-EP, and their corresponding polycarbonates, P-TEP$_x$CN$_y$ ($x = 0$, 1, 2, 4, 30, 120; $y = 0$, 1) in aggregate and solution states were studied. As shown in Figs. 2a and b and Fig. S18 (Supporting information), bright luminescent colors of polycarbonates change from yellow to blue with the gradual increase in the proportion of TPE-EP doping. The absorption spectra of these samples in THF solutions with a concentration of 1.0×10^{-5} mol/L, also confirm the successful preparation of the corresponding polycarbonates. All of these polymers show similar absorption spectra which give two or three absorbance peaks in the region of 200–500 nm. The peak that appeared at 250 nm for these samples could be assigned to the polymer backbone, while the other obvious peak that appeared at 310 nm is attributed to the TPE unit, and the absorbance peak at about 400 nm could be assigned to the portion contained cyano unit. Meanwhile, the absorption of high concentration aggregated state shows the same trend (Fig. S19 in Supporting information). To verify the AIE properties of the two monomers and resulting copolymers, their emission behavior was measured in THF/water system. As shown in Figs. S20 and S21 (Supporting information), TPE-EPCN shows obvious AIE behavior when excited at 365 nm with an emission peak at 560 nm. When $f_w = 0$ to 60%, it shows almost no emission in the system and then enhances quickly as f_w increases from 70% to 90% to exhibit bright red-orange emission. TPE-EP exhibits similar behavior as that of TPE-EPCN. While $f_w \leq$ 80%, the emission peak in the range of 410–440 nm is attributed to pure THF solution. As the continuous increase of water fraction, the emission intensity reaches its highest value and bright blue light emission is obtained.

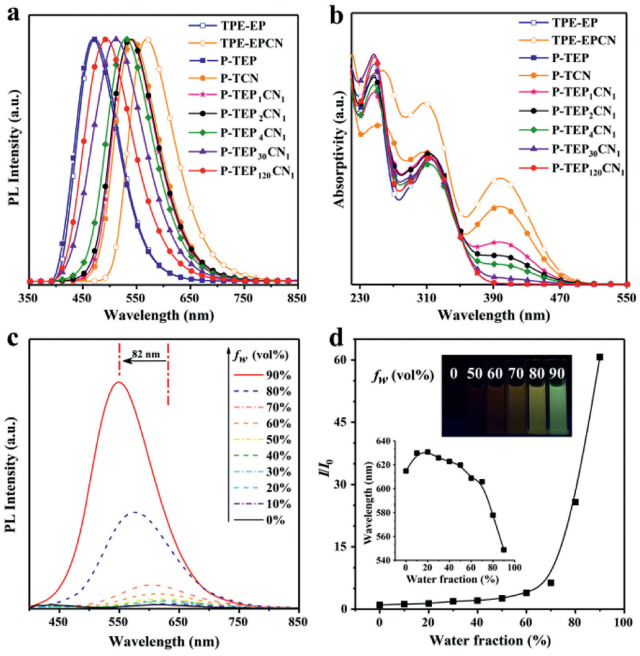

Fig. 2. (a) Emission spectra, (b) absorption spectra of TPE-EP, TPE-EPCN and P-TEP$_x$CN$_y$ ($x = 0$, 1, 2, 4, 30, 120; $y = 0$, 1). (c) PL intensity changes in THF/water mixtures with different water volume fractions (f_w) of P-TEP$_1$CN$_1$. (d) Plot of relative PL intensity (I/I_0) *versus* f_w of the THF/H_2O mixture of P-TEP$_1$CN$_1$. Inset of (d): fluorescence photos at corresponding f_w and the wavelength of the nanoaggregates of P-TEP$_1$CN$_1$ formed in THF/H_2O mixtures with various water fractions.

As for the several corresponding polymers, P-TEP shows the same emission behavior as that of blue light-emitting TPE-EP. The other six polymers also show obvious AIE properties with similar trends in THF/H_2O system. Among them, when excited at 365 nm, P-TEP$_1$CN$_1$ shows non-emission in pure THF solution (Figs. 2c and d), while upon the addition of distilled water, when $f_w = 90\%$, the fluorescence intensity of P-TEP$_1$CN$_1$ reaches its maximum value with nearly 60 times higher than that when $f_w = 0\%$. Meanwhile, a clear blue shift emission of about 82 nm is also observed when f_w > 50%. This is attributed to their poor solubility in water, aggregates are gradually formed and precipitated when the percentage of f_w increases by degrees, which are less polar in aggregates than in THF solution, resulting in a blue-shift of its fluorescence [53]. Other copolymers with different dropping ratios show the same emission behavior (Figs. S22-S27 in Supporting information). Additional photophysical data such as lifetime and quantum efficiency are summarized in Table S1 (Supporting information).

Benefiting from their bright emission, we further explored their application in solid-state white light-emitting materials. Based on the excitation and emission spectra of several polymers, we selected P-TCN, with the most suitable peak position, as a phosphor for the construction of a white light-emitting diode (WLED). TGA and DSC curves of P-TCN were measured and shown in Fig. S28 (Supporting information). The above results show that P-TCN has good stability, and it is suitable for the application of LED devices.

As shown in Fig. 3a, P-TCN is coated on the surface of the commercial blue light-emitting chip ($\lambda_{em} = 460$ nm). Immediately, bright white light emission can be observed when the power is switched on, with CIE coordinate of (0.32, 0.32) (Figs. 3b and c), which is very close to the pure white light (0.33, 0.33) [54]. It shows 51.20 cd/A for correlated current efficiency (CE), 56.08 lm/W for luminescent efficiency (LE), and 26.09% for external quantum efficiency (EQE), along with 5997 K for color temperature (CCT) and 77 for color rendering index (CRI), indicating the successful fabrication of WLED device. For practical application (Fig. 3a, right), as power is switched on, the colors of these roller pens are visible under the illumination of the fabricated WLED light source with similar colors compared to those under daylight.

Fluorescence detection of explosives, including, 2,4,6-trinitrophenol (TNP), 2,4-dinitrotoluene (DNT), dinitrobenzene

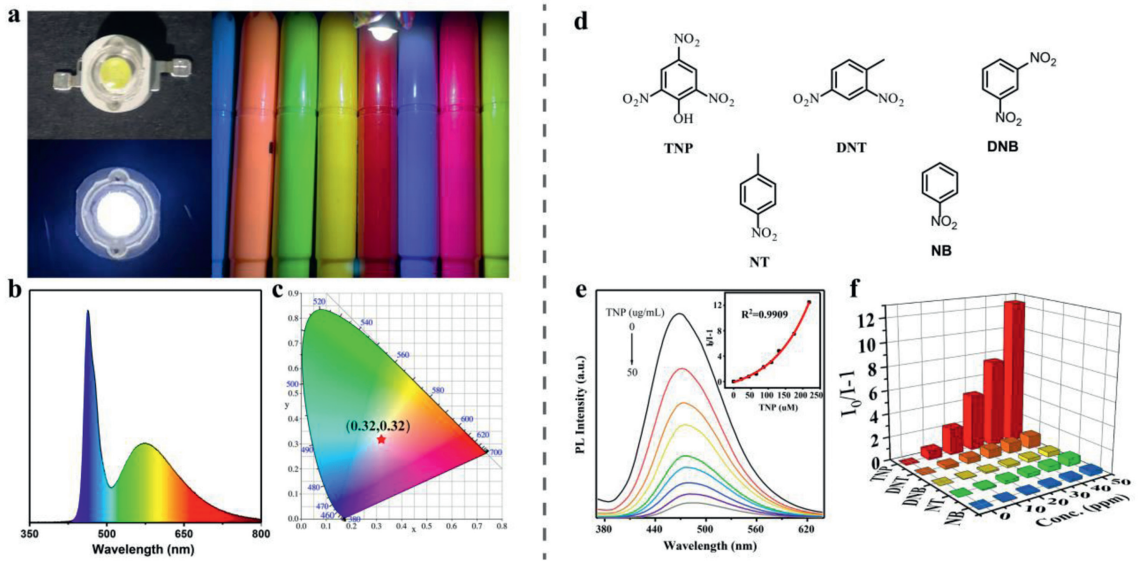

Fig. 3. (a) Photograph of LED device coated with P-TCN (left) and color state of the watercolor pen under WLED on (right). (b) EL spectra of the resultant device. (c) CIE chromaticity diagram of P-TCN coated LED device. (d) Analytes used in the present research. (e) Emission spectra of P-TEP in THF/H_2O system ($f_w = 90\%$) in the presence of different concentrations of TNP. Inset: Stern-Volmer plot of I_0/I-1 *versus* TNP concentration in aqueous solution upon the addition of nitroaromatics. $\lambda_{ex} = 350$ nm. Concentration: 100 μg/mL. (f) Three-dimensional SV histogram of various nitroaromatics.

(DNB), 4-nitrotoluene (NT) and nitrobenzene (NB) was explored through a series of fluorescence quenching experiments using the emissive polymer nanoaggregates THF/H_2O mixtures (1:9, v/v) as fluorescence probes because of its strong light emissions. TNP was selected as a model analyte due to its economic advantages. Fig. S29 (Supporting information) shows the UV absorption spectrum of explosives and emission spectra of polymer nanoaggregates, a definite overlap could be observed for polymer P-TEP, P-$TEP_{120}CN_1$, and nitroaromatics TNP, which suggested the occurrence of resonance energy transfer. As shown in Figs. 3d-f and Fig. S30 (Supporting information), the fluorescence of P-TEP, P-$TEP_{120}CN_1$ nanoaggregates could be efficiently quenched after the addition of explosives. For P-TEP, when 50 ug TNP, DNT, DNB, NT and NB were added, their fluorescence quenching efficiencies reached 93%, 52%, 29%, 40% and 27%, respectively. In addition, for P-$TEP_{120}CN_1$, when 40 μg nitroaromatics were added, their fluorescence quenching efficiencies reached 94%, 40%, 25%, 37% and 8%, respectively. To sum up, the fluorescence quenching efficiencies of both P-TEP, P-$TEP_{120}CN_1$ nanoaggregates are in the order of TNP > DNT > NT > DNB > NB. The Stern-Volmer plots of the two polymers show a tendency to bend upwards instead of linear lines, giving the corresponding quenching constants of 2.48×10^4 and 2.33×10^4 mol/L, respectively, implying their certain sensitivity to nitroaromatics, especially, polynitrophenol aromatic compounds.

In conclusion, we reported a facile design strategy to prepare AIE polymers with tunable emission color, and successfully synthesized a series of biodegradable polycarbonates P-TEP_xCN_y ($x = 0$, 1, 2, 4, 30, 120; $y = 0$, 1) with well-defined structures and particular photophysical properties through the alternating copolymerization of CO_2 and propylene oxide (PO) under SalenCo(III)Cl/PPNCl catalyst system. On the other hand, tetraphenylethylene derivatives, TPE-EP and TPE-EPCN were grafted onto side chains of the polycarbonate backbones to endow the resulting polymers with AIE proprieties. In terms of applications, we have successfully prepared high-performance WLED using P-TCN with a luminescence efficiency of 56.08 lm/W and external quantum efficiency of 26.09%. In addition, P-TEP and P-$TEP_{120}CN_1$ in their aggregated states can be used as probes for the effective and selective detection of nitroaromatic explosives in aqueous solutions.

Declaration of competing interest

The authors declare that they have no known competing financial interests or personal relationships that could have appeared to influence the work reported in this paper.

Acknowledgments

This work was supported by the National Natural Science Foundation of China (No. 22175033) and the Scientific and Technological Innovation Team of Shanxi Province (No. 2022TD-36).

References

[1] X. Jing, P. Feng, Z. Chen, et al., ACS Sustain. Chem. Eng. 9 (2021) 9209–9220.
[2] C.M. Boutry, A. Nguyen, Q.O. Lawal, et al., Adv. Mater. 27 (2015) 6954–6961.
[3] C.M. Boutry, Y. Kaizawa, B.C. Schroeder, et al., Nat. Electron. 1 (2018) 314–321.
[4] S.V. Patil, S.S. Shelake, S.S. Patil, Polymeric materials for targeted delivery of bioactive agents and drugs, in: S. Thomas, P. Balakrishnan, M.S. Sreekala (Eds.), Fundamental Biomaterials: Polymers, Woodhead Publishing, 2018, pp. 249–266.
[5] N.H. Yusoff, K. Pal, T. Narayanan, F.G. De Souza, J. Mol. Struct. 1232 (2021) 129954.
[6] M. Luo, A.W. Martinez, C. Song, et al., J. Microelectromech. Syst. 23 (2014) 4–13.
[7] B.Y. Peng, Z. Chen, J. Chen, et al., Environ. Int. 145 (2020) 106106.
[8] H.C. Wang, J.M. Grolman, A. Rizvi, et al., ACS Macro Lett 6 (2017) 321–325.
[9] S.S. Yang, M.Q. Ding, L. He, et al., Sci. Total Environ. 756 (2021) 144087.
[10] J.M. Jeon, S.J. Park, T.R. Choi, et al., Polym. Degrad. Stab. 191 (2021) 109662.
[11] M.L. Wang, E.H. Wang, H. Cao, et al., Chin. J. Chem. 39 (2021) 3037–3043.
[12] B. Grignard, S. Gennen, C. Jerome, et al., Chem. Soc. Rev. 48 (2019) 4466–4514.
[13] S. Klaus, M.W. Lehenmeier, C.E. Anderson, B. Rieger, Coord. Chem. Rev. 255 (2011) 1460–1479.
[14] Y. Zhu, C. Romain, C.K. Williams, Nature 540 (2016) 354–362.
[15] Y. Qin, X. Sheng, S. Liu, et al., J. CO_2 Util. 11 (2015) 3–9.
[16] S. Ye, S. Wang, L. Lin, et al., Adv. Ind. Eng. Polym. Res. 2 (2019) 143–160.
[17] G.P. Wu, P.X. Xu, X.B. Lu, et al., Macromolecules 46 (2013) 2128–2133.
[18] K. Bauri, B. Saha, A. Banerjee, P. De, Polym. Chem. 11 (2020) 7293–7315.
[19] B. Liu, H. Zhang, S. Liu, et al., Mater. Horiz. 7 (2020) 987–998.
[20] J.Q. Liu, Z.D. Luo, Y. Pan, et al., Coord. Chem. Rev. 406 (2020) 213145.
[21] K. Wang, K. Amin, Z. An, et al., Mater. Chem. Front. 4 (2020) 1803–1915.
[22] S. Zhang, D. Liu, G. Wang, Molecules 27 (2022) 2586.
[23] Y.N. Jing, S.S. Li, M. Su, et al., J. Am. Chem. Soc. 141 (2019) 16839–16848.
[24] C. Wang, Z. Wang, S. Chen, et al., Macromol. Rapid Commun. 42 (2021) e2100264.
[25] W. Huang, E. Smarsly, J. Han, et al., ACS Appl. Mater. Interfaces 9 (2017) 3068–3074.
[26] C. Wang, Z. Li, Mater. Chem. Front. 1 (2017) 2174–2194.

[27] Y. Huang, J. Xing, Q. Gong, et al., Nat. Commun. 10 (2019) 169.
[28] J. Luo, Z. Xie, J.W. Lam, et al., Chem. Commun. (2001) 1740–1741.
[29] D. Ding, K. Li, B. Liu, B.Z. Tang, Acc. Chem. Res. 46 (2013) 2441–2453.
[30] J. Mei, N.L.C. Leung, R.T.K. Kwok, et al., Chem. Rev. 115 (2015) 11718–11940.
[31] Z. Meng, H. Xue, T. Wang, et al., J. Nanobiotechnol. 20 (2022) 344.
[32] X. Zhai, R. Chen, W. Shen, TrAC, Trends Anal. Chem. 146 (2022) 116502.
[33] S. Ge, E. Wang, J. Li, B.Z. Tang, Macromol. Rapid Commun. 43 (2022) e2200080.
[34] E.H. Wang, S.J. Liu, J.W.Y. Lam, et al., Macromolecules 53 (2020) 5839–5846.
[35] J. Huang, H. Qin, H. Liang, J. Lu, Polymer (Guildf) 202 (2020) 122663.
[36] Z. Wang, N. Wang, H. Gao, et al., Analyst 145 (2019) 233–239.
[37] Y. Zhang, P. Shen, B. He, et al., Polym. Chem. 9 (2018) 558–564.
[38] B. Wang, C. Li, L. Yang, et al., J. Mater. Chem. B 7 (2019) 3846–3855.
[39] J. Zhang, W. Liang, L. Wen, et al., Biomater. Sci. 9 (2021) 5293–5301.
[40] H. Liu, Z. Hu, H. Zhang, et al., Angew. Chem. Int. Ed. 61 (2022) e202203505.
[41] J. Yang, X. Yu, J.I. Song, et al., Angew. Chem. Int. Ed. 61 (2022) e202115208.
[42] Z. Cong, S. Xie, Z. Jiang, et al., Chem. Eng. J. 431 (2022) 133748.
[43] S. Wang, W. Wu, P. Manghnani, et al., ACS Nano 13 (2019) 3095–3105.
[44] M. Kang, Z. Zhang, N. Song, et al., Aggregate 1 (2020) 80–106.
[45] X.Y. Lou, G. Zhang, N. Song, Y.W. Yang, Biomaterials 286 (2022) 121595.
[46] Z. Zhang, M. Kang, H. Tan, et al., Chem. Soc. Rev. 51 (2022) 1983–2030.
[47] L. Feng, C. Li, L. Liu, et al., Angew. Chem. Int. Ed. 61 (2022) e202212673.
[48] B. He, S. Ye, Y. Guo, et al., Sci. China Chem. 56 (2013) 1221–1227.
[49] Z. Liu, S. Hu, L. Zhang, et al., Sci. China Chem. 56 (2013) 1129–1136.
[50] D. Wu, T. Zhang, J. Sun, et al., Tetrahedron 74 (2018) 7218–7227.
[51] W. Wu, S. Ye, R. Tang, et al., Polymer (Guildf) 53 (2012) 3163–3171.
[52] S. Shao, L. Wang, Aggregate 1 (2020) 45–56.
[53] L. Zhu, C. Yang, J. Qin, Chem. Commun. (2008) 6303–6305.
[54] X. Chen, J. Chen, G. Sun, et al., ACS Appl. Mater. Interfaces 13 (2021) 38629–38636.